Excited-State Dynamics of Isolated DNA Bases: A Case Study of Adenine

Christer Z. Bisgaard,[b] Helmut Satzger,[b] Susanne Ullrich,*[a] and Albert Stolow*[b]

We present a summary of recent advances in the understanding of the UV photophysics of the isolated DNA base adenine, emphasizing a discussion of the mechanisms behind the ultrafast relaxation following excitation to the ππ* band. Drawing on our femtosecond time-resolved photoelectron spectroscopy experiments, we discuss differences in the ultrafast relaxation of adenine and 9-methyladenine and consider the relative merits of the various proposed mechanisms.

1. Introduction

The ultraviolet photostability of biomolecules such as DNA is generally determined by excited-state electronic relaxation processes. Ultraviolet excitation within DNA can lead to singlet excited-state photochemistry and, hence, potential mutagenic damage.[1] Although intracellular DNA repair mechanisms exist, these are relatively slow and energetically inefficient. Therefore, molecular features that lead to any intrinsic photostability will have an advantage. What determines this intrinsic photostability? Generally, excited states of molecules have—due to their altered charge distributions—much higher reactivities than ground states. As such, electronically excited states must be considered dangerous to biomolecules, since any ensuing photochemistry could alter their nature and, hence, function. Mechanisms which quench or relax the electronically excited state back to the ground state are important photostabilization mechanisms. In molecules, this electronic relaxation is achieved by the non-adiabatic processes variably named internal conversion or radiationless transition.[2] These convert dangerous electronic energy into less dangerous vibrational energy, the latter being cooled efficiently in aqueous solution. However, in order to be effective, these non-adiabatic mechanisms must operate on ultrafast time scales in order to dominate over competing ultrafast photochemical mechanisms that potentially damage the biomolecule. This leads to the suggestion that molecules such as DNA might have ultrafast internal conversion dynamics which rapidly evolve the UV excited state back to the ground state. Within DNA, the UV chromophores are the aromatic nucleobases themselves and their photophysics within DNA determines the outcome of UV absorption. The formation of excimers within a single strand seems to be an important damage mechanism, but one that is well-suited to repair.[3] Even the isolated DNA base adenine, the focus of recent debate, reveals ultrafast electronic relaxation mechanisms.[1,4–10] The details of the non-adiabatic dynamics within adenine remain under discussion, although much progress has been made. Our purpose herein is to consider, as a case study, the primary photophysics of isolated adenine, drawing primarily from our own efforts which are based on time-resolved photoelectron spectroscopy (TRPES).

Time-resolved photoelectron spectroscopy has recently been reviewed in some detail[11–13] and therefore we only summarize here. Since photoelectron spectroscopy is sensitive to both electronic configurations and vibrational dynamics, TRPES is particularly useful for studying excited-state non-adiabatic dynamics. Due to the range of symmetries of the outgoing electron, photoionization is always an allowed process and, therefore, there are no "dark" states in TRPES. Moreover, as a dispersed as opposed to integrated measurement technique, it provides more information than time-resolved photo-ion detection, the analogy for photon detection being the advantage of dispersed fluorescence over total fluorescence. Briefly, the method involves pumping an isolated molecule to an excited state with an ultrashort pump laser pulse. After a variable time delay, an ultrashort probe laser pulse ionizes the excited state and the resultant photoelectrons are measured as a function of time. This photoelectron spectrum provides information about the overlap between the evolving excited state and the set of electronic states of the cation. By making use of Koopmans' ionization correlations, the electronic dynamics can be disentangled from the vibrational dynamics,[14] allowing a direct view of the various configurations that the molecule passes through during its evolution.

Below, we briefly review the photophysics of isolated adenine, with emphasis on its optical spectroscopy. Then we give an overview of the ab initio calculations that have been carried out on the molecule, and of the proposed relaxation mecha-

[a] Dr. S. Ullrich
Department of Physics and Astronomy
University of Georgia, Athens, GA, 30602-2451 (USA)
Fax: (+1) 706-542-2492
E-mail: ullrich@physast.uga.edu

[b] Dr. C. Z. Bisgaard, Dr. H. Satzger,+ Dr. A. Stolow
Steacie Institute for Molecular Sciences
Ottawa, ON, K1A 0R6 (Canada)
Fax: (+1) 613-991-3437
E-mail: albert.stolow@nrc.ca

[+] Current address:
Leibniz Supercomputing Centre
Boltzmannstr. 1, 85748 Garching (Germany)

nisms that have emerged. We then turn to the results of experiments aimed at unravelling the relaxation mechanisms following optical excitation: femtosecond time-resolved mass spectrometry, high translational energy resolution hydrogen atom detection and femtosecond time-resolved photoelectron spectroscopy.

2. Introduction to the Photophysics of Adenine

The purine bases adenine and guanine and the pyrimidine bases cytosine, thymine, and uracil are the basic building units for DNA and RNA. All the bases are heterocycles and have a number of tautomers and, additionally, each of the imino tautomers can exist as *E* and *Z* stereoisomers. The bases typically have strong $\pi\pi^*$ UV absorption bands and, due to the large number of lone electron pairs, additional low-lying $n\pi^*$ states. Furthermore, for some bases $\pi\sigma^*$ states may also be in a similar energy range. One can anticipate that this leads to complex photophysical properties and poses a tremendous challenge to ab initio calculations. Of the five bases, adenine has been studied most extensively by both frequency- and time-resolved gas-phase experiments and quantum chemical electronic structure calculations.

The lowest energy and most abundant gas-phase tautomer of adenine is the 9H-form[15] shown in Figure 1; our discussion refers to this structure, unless otherwise stated. Vertical and
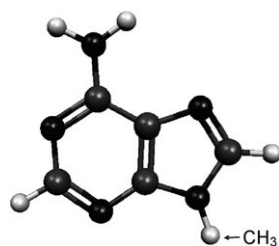

Figure 1. 9H form of adenine. Methylation of the N9H group is indicated which leads to 9-methyladenine.

adiabatic transition energies for adenine's lowest singlet excited states have been calculated at different levels of theory (see for instance Table 4 of ref. [1] and Table 1 of ref. [16]). Whereas most theoretical methods agree that there are two nearby low-energy singlet $\pi\pi^*$ states (referred to as ^1L_a and ^1L_b), there has been some disagreement regarding the relative location of the dark $n\pi^*$ state in the Franck–Condon region. For example, scaled configuration interaction singles (CIS) and complete active space with second-order perturbation theory (CASPT2) calculations have predicted that the lowest $n\pi^*$ state is energetically above the $\pi\pi^*$ states[4,17–19] whereas time dependent density functional (TD-DFT) calculations using the B3LYP functional find that the $n\pi^*$ state is lowest in energy.[6,20] This point has been important to settle as the dark $n\pi^*$ and $\pi\sigma^*$ states could play a role in the ultrafast internal conversion following excitation to the optically bright $\pi\pi^*$ state. Recent high-level

ab initio calculations predict the $n\pi^*$ state to be below the $\pi\pi^*$ state and thus removes the controversy.[21,22]

3. UV Spectroscopy

Early vapor phase spectra of adenine and 9-methyladenine recorded by Clark et al.[23] (Figure 2) show a $\pi\pi^*$ absorption band with a maximum around 252 nm and 249 nm for adenine and 9-methyladenine, respectively. For adenine a second, stronger peak around 207 nm was determined; 9-methyladenine too has strong absorption in this wavelength region. The authors attribute the absence of indications of an $n\pi^*$ state to the generally low intensity of $n\pi^*$ transitions or that it might be hidden under the $\pi\pi^*$ transition.
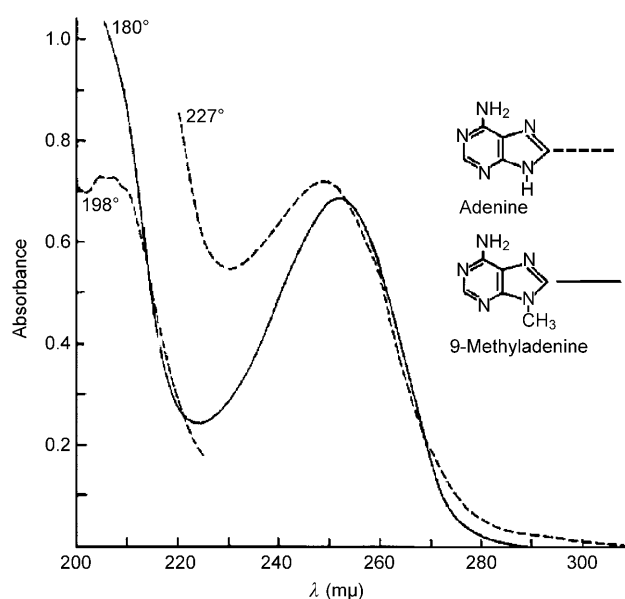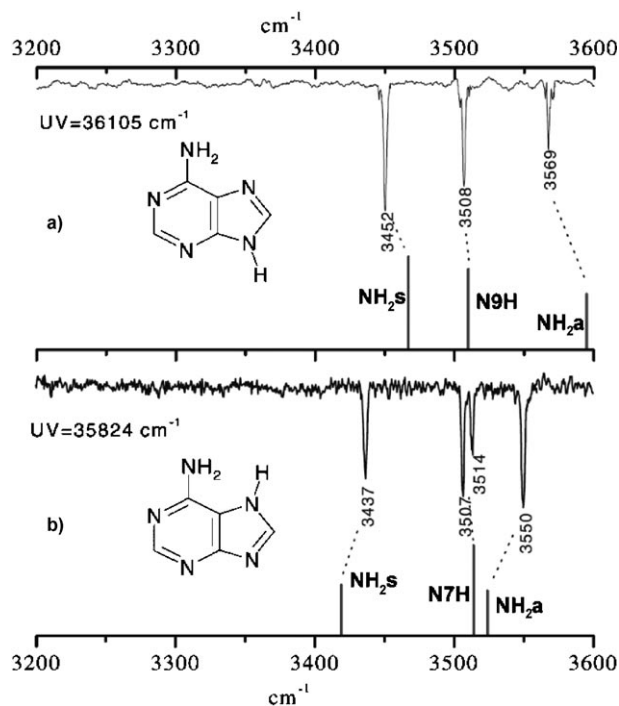

Figure 2. Vapor-phase absorption spectra of adenine and 9-methyladenine. Reproduced with permission from ref. [23]. Copyright 1965, American Chemical Society.

Spectroscopies, such as resonance-enhanced multi-photon ionization (REMPI) and laser-induced fluorescence (LIF) in cold molecular beams provide details that cannot be resolved in room-temperature experiments. In the case of adenine, valuable information about the low-energy region of the absorption band is contained in the observation of discrete vibronic transitions near 36 000 cm^{-1} (278 nm) by Kim et al.[24] (see Figure 3). In agreement with others,[25–28] the transition at 36 108 cm^{-1} (peak D) was assigned to the origin of the singlet $\pi\pi^*$ transition. Smaller features below the S_2 $\pi\pi^*$ origin have been controversial and their interpretation complicated by the possible presence of different tautomers in the molecular beam. A powerful tool to overcome these difficulties is the use of IR–UV double-resonance techniques in conjunction with quantum chemical calculations.[29] Kleinermanns and co-workers[26,27] demonstrated in such double-resonance experiments that the weak band labelled A originates from a dark $n\pi^*$ tran-
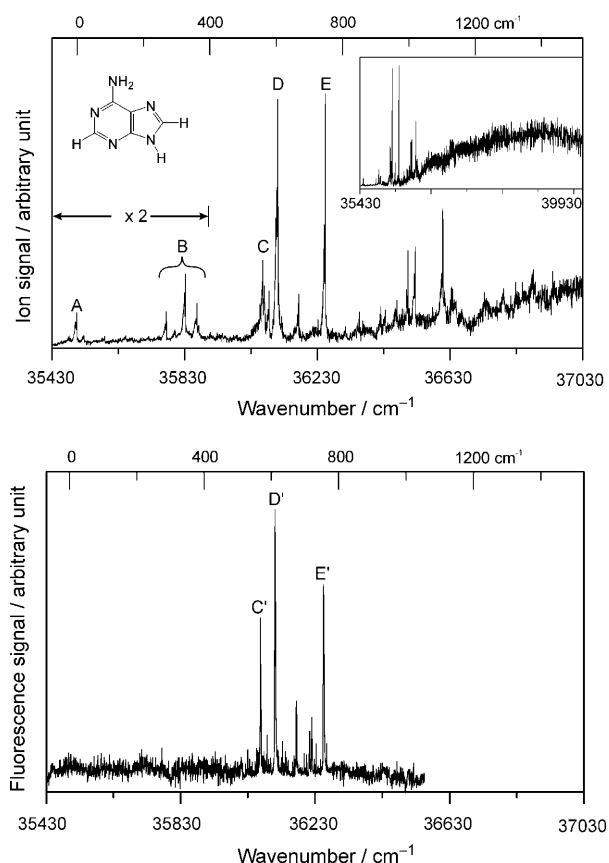
Figure 3. One-color REMPI spectrum (top) and fluorescence excitation spectrum (bottom) of adenine. The peak D is assigned to the origin of the lowest ππ* band. Reused with permission from ref. [24]. Copyright 2000, American Institute of Physics.

Figure 4. IR–UV double resonance spectrum of adenine recorded with the UV probe laser tuned to a) 36 105 cm⁻¹ and b) 35 824 cm⁻¹ and the IR laser tuned over the NH₂ and NH stretch region. The line spectra show ground-state vibrational frequencies calculated at the B3LYP/6-311G(d,p) level of theory. Reproduced from ref. [26] with kind permission of The European Physics Journal (EPJ).

sition in 9H-adenine, whereas peak B can be attributed to the presence of 7H-adenine in the molecular beam. In Figure 4 we show the IR–UV double resonance spectra recorded with the UV probe laser tuned to a) 36 105 cm⁻¹ (peak D) and b) 356 824 cm⁻¹ (peak B), respectively, and the IR laser scanned over the NH₂ and N–H stretch region. The IR dip pattern in the REMPI signal is compared to B3LYP/6-311G(d,p) vibrational frequencies of the ground state symmetric and antisymmetric NH₂ stretch and the N9H/N7H stretches (Figure 4, line spectra). The IR dip spectrum of peak B at 35 824 cm⁻¹ shows NH₂ stretch frequencies shifted to slightly lower energies, as predicted for 7H-adenine; this UV transition therefore originates from the 7H-tautomer. The IR dip spectra of peak D at 36 105 cm⁻¹ and peak A at 35 497 cm⁻¹ are identical and match the vibrational frequencies of 9H-adenine. As peak A occurs energetically below the ππ* origin, it was assigned to the nπ* state of 9H-adenine. The unexpected intensity of the dark nπ* peak was explained by extensive mixing with the strongly allowed ππ* transition. These spectrally resolved studies confirmed the close proximity of a ππ* and nπ* state as predicted by theory, but no clear evidence for a second low-lying singlet ππ* state was found. Importantly, the REMPI and LIF spectra of adenine show only a few resolved features. At higher excitation energies, the REMPI spectrum evolves into a broad, struc-

tureless band and no fluorescence is detected. These observations are indicative of fast non-radiative excited-state relaxation dynamics.

4. Theoretical Models

Two qualitatively different models for the primary photophysics of isolated adenine have been proposed (see Figure 5). Broo[4] suggested that a nearly barrierless path along a six-membered ring-puckering reaction coordinate connects the initially excited ππ* state to the ground state via the nπ* state. Whereas the ππ* state has the lowest vertical excitation energy, the nπ* state was found at even lower energies along the ring puckering path. At excitation energies above the band origin, Domcke and Sobolewski[22] proposed an alternative mechanism involving a conical intersection of the optical bright ππ* state with the repulsive and optically dark πσ* state, followed by decay back to the S₀ ground state via another conical intersection at a large N9–H bond distance. This reaction path is almost barrierless and is expected to be highly efficient, due to the repulsive character of the πσ* state and the small inertia involved in the N–H stretching motion.

Several groups have used ab initio calculations to investigate the primary photophysics of adenine, in particular that of the 9H-tautomer. Perun et al.[30] examined two additional pathways accessible from the Franck–Condon region, namely opening of the five-membered ring; and N–H dissociation from the
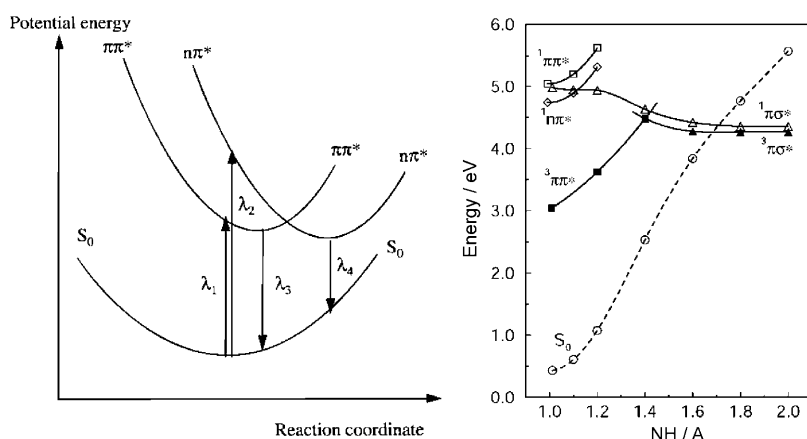
Figure 5. Relaxation pathways from the optically bright $\pi\pi^*$ state to the electronic ground state have been predicted along a 6-membered ring puckering motion by Broo[4] (left) and along the N(9)-H stretch coordinate by Sobolewski and Domcke[22] (right). Reproduced from ref. [4] (Copyright 1998, American Chemical Society) and ref. [22] with kind permission of The European Physics Journal (EPJ).

amino group. While opening of the ring involves the passage over a large barrier, dissociation from the amino group involves only a small barrier and is accessible at energies similar to the N9–H dissociation channel. The latter conclusion is supported by the calculations of Marian[31] who also noted that the N–H dissociation channels are only energetically accessible in a strictly planar geometry.

Much attention has been given to the complex topography of the lowest $\pi\pi^*$ and $n\pi^*$ states.[16,21,31–34] The proximity of three excited states, which are strongly coupled at some geometries, makes this a very interesting and challenging problem involving several conical intersections and switching between the electronic states. Furthermore, dynamic electron correlation seems to cause significant shifts in the relative energy amongst these states, thus necessitating the use of high-level models and a careful choice of basis set and active space to ensure a balanced treatment of all states. Of the three states involved, the $\pi\pi^*$ state ^1L_a is agreed to have the largest oscillator strength, but it is also the $\pi\pi^*$ state with the highest vertical excitation energy. Irrespective of the relative ordering of the $\pi\pi^*$ states and the $n\pi^*$ state at the S_0 equilibrium geometry, all methods agree that the $n\pi^*$ state has the lowest-lying local minimum, in agreement with the assignment of the REMPI and LIF spectra in Figure 3. They also agree that a conical intersection between the ^1L_a $\pi\pi^*$ state and S_0 exists at energies below this minimum. While the details of the state mixing and, thus, the precise position of transition states, depends on the model chosen, there seems to be consensus that out-of-plane twisting of the C2 atom in the six-membered ring provides a direct path with little or no barrier from the ^1L_a state in the Franck–Condon region to S_0. The lack of quantitative agreement between even very similar methods led Zgierski et al.[16] to point out the high degree of qualitative agreement between the calculations and highlighted the similarity between the path involving C2 out-of-plane twisting and the well-known biradical mechanism for radiationless decay in benzene and ethylene. A second common path involves coupling

from the $\pi\pi^*$ states to the $n\pi^*$ state followed by a twisting of N1 and C6 out of the plane of the six-membered ring, whereby a low-lying conical intersection with S_0 is reached. This path, however, has a significant barrier along the twisting coordinate. More paths involving other crossings between the $\pi\pi^*$ and $n\pi^*$ states have been identified, but are not detailed here.

Quantum chemical ab initio and DFT calculations have made considerable progress in characterizing excited-state potential energy surfaces by identifying specific points such as minima, transition states, barrier heights, conical intersections and the pathways connecting them. The calculations on adenine summarized above provide extremely valuable insight into adenine's electronic structure. Given the large number of degrees of freedom in this complex molecule, it is not surprising that a number of potential relaxation pathways along different coordinates have been suggested. The actual significance and branching ratios of specific, energetically accessible pathways, however, can only be determined by rather challenging dynamics calculations[35,22] or by carefully designed experiments.

5. Experiments

A variety of time- and spectrally-resolved experimental techniques have been employed to determine which of the proposed relaxation pathways contribute to the photophysics of adenine. Unfortunately, the optically dark and repulsive $\pi\sigma^*$ states are difficult to detect spectroscopically, but indirect evidence can be obtained through substitution and H-atom detection experiments. Since relaxation via the $\pi\sigma^*$ state is localized at the N9-H bond, substitution of this H-atom with the more strongly bound methyl group is expected to perturb this relaxation path. Indeed, quantum chemical calculations indicate that for 9-methyladenine a conical intersection between the $\pi\sigma^*$ state and the ground state might not be present.[42] It was therefore argued that if the $\pi\sigma^*$ state plays an important role, the excited state lifetime should be longer for 9-methyladenine than for adenine. The first time-resolved ion yield measurements, with 267 nm pump and 800 nm multi-photon probe, showed a 1 ps single exponential decay for both adenine and 9-methyladenine at 400 fs time resolution.[5,36] More recently, an ion yield study with a higher time resolution of 80 fs, by Canuel et al.[7] revealed a double-exponential decay with 100 fs and 1.1 ps components instead (see Figure 6). Upon N9-methylation these lifetimes were found to be 110 fs and 1.3 ps, essentially unchanged. This was taken as indirect evidence that the $\pi\sigma^*$ state does not play a significant role in the decay of the initially excited state. Instead, relaxation via
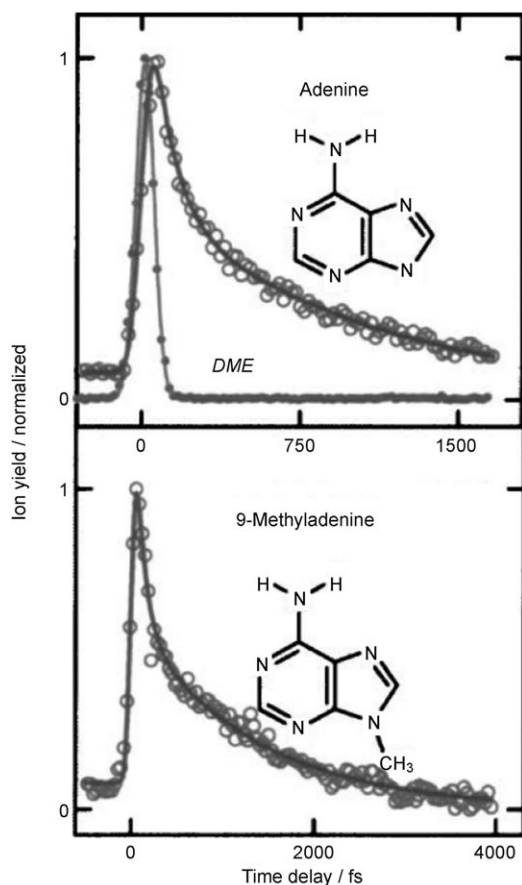
Figure 6. Time-resolved ion yield measurements of adenine and 9-methyladenine recorded at 266 nm excitation and two photon probe at 400 nm. Reused with permission from ref. [7]. Copyright 2005, American Institute of Physics.

the $n\pi^*$ state was proposed as the most likely pathway. As described below, other experiments have revealed significant differences between the dynamics in adenine and 9-methyladenine, thus challenging this conclusion.

6. Hydrogen Loss

Relaxation via the $\pi\sigma^*$ state involves large-amplitude motion along the N9-H bond. At nearly twice the equilibrium distance, there is a conical intersection between the $\pi\sigma^*$ state and the ground state. The dynamics through this conical intersection determines if relaxation via the $\pi\sigma^*$ state leads to direct dissociation of the N9-H bond or to high-lying vibrational states in

the electronic ground state. None of the other proposed relaxation mechanisms involve large-amplitude motion of the hydrogen atom. Observation of hydrogen atoms with a fast and peaked velocity distribution and a short appearance time following UV excitation can therefore be considered an indirect proof for relaxation along a $\pi\sigma^*$ state. One has to keep in mind, however, that hydrogen atom detection is a very sensitive technique and can reveal even very small quantum yields. The observation of hydrogen atoms by Hünig et al.[37] and Zierhut et al.[38] provided a compelling argument for the participation of the $\pi\sigma^*$ state: H-atom appearance times, Doppler profiles and the comparison of H-atom loss signals from adenine and 9-methyladenine confirmed that the H-atoms predominantly originated from the azine group. In Figure 7 (left), we show the mass spectra of adenine and 9-methyladenine recorded by Zierhut et al.[38] with and without 239.5 nm light for excitation, using a [1+1′] resonant two-photon ionization probe scheme (121.6 nm + 365 nm) to detect hydrogen atoms. Without UV excitation, the H-atom signal is negligible for both adenine and 9-methyladenine. However, the signal increases significantly with the excitation pulse. Even though the parent ion signal of the adenine and 9-methyladenine molecules are of comparable size, the H-atom signal originating from 239.5 nm excitation is considerably smaller in 9-methyladenine. This indicates that dissociation of the N9-H bond in adenine presents a major contribution to the observed H-atom signal. Similar mass spectra are observed for 266 nm excitation. A time-delay scan between the 266 nm excitation and 121.6 nm H-atom detection reveals rate constants of $>4\times10^8$ s^{-1} (corresponding to an appearance time of <2.5 ns) and $>2.5\times10^8$ s^{-1} for adenine and 9-methyladenine, respectively. These values represent a lower limit, due to the nanosecond time-resolution of Zierhut et al.'s experimental setup. In Figure 7 (right), we show Doppler profiles of the ejected H-atoms fol-
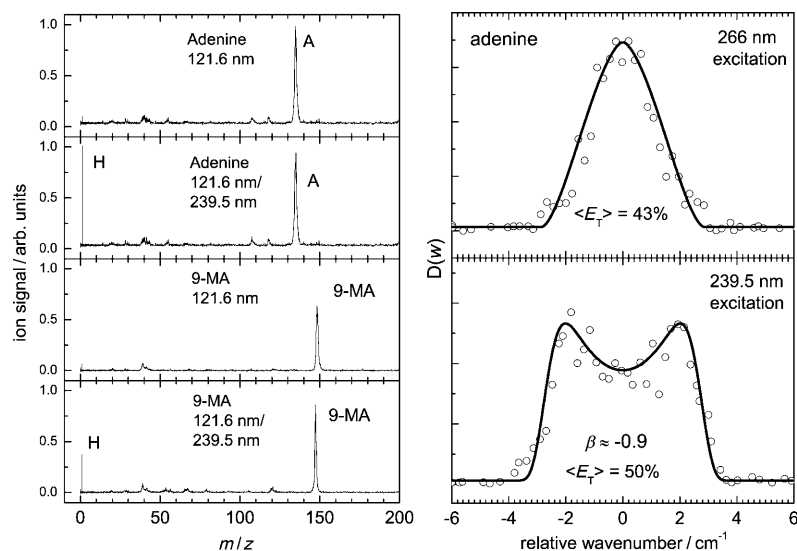
Figure 7. Left: Mass spectra of adenine and 9-methyladenine recorded with 121.6 nm + 365 nm ionization with or without prior excitation at 239.5 nm. Right: Doppler profiles of H-atoms released from adenine excited at 266 nm (top) or 239.5 nm (bottom). In both cases the H-atom carries a large fraction of the available energy as kinetic energy, indicative of direct dissociation.[38] Reproduced with permission from the PCCP Owner Societies.

lowing 266 nm (top) and 239.5 nm (bottom) excitation of adenine at a pump–probe delay of 10 ns. The fact that an anisotropic Doppler profile is observed at 239.5 nm confirms that H-atom ejection must occur on a significantly shorter time scale than a rotational period, that is, within picoseconds of the excitation. A dissociation energy of 393 ± 20 kJ can be approximated from the maximum frequency shift observed in the Doppler profile which represents the maximum speed or kinetic energy of the ejected H-atoms. Further analysis showed that approximately 50 % of the available energy is released into the translation energy of the H-atoms. At longer wavelengths Zierhut et al. (266 nm) and Hünig et al. (243.1 nm) both observed Doppler profile that indicate an isotropic emission of hydrogen atoms, indicative of a change in the mechanism in this wavelength region. More recently Nix et al.[39] reported high-resolution total kinetic energy release (TKER) spectra of H-atom fragments resulting from photodissociation of jet-cooled adenine molecules using a similar probe scheme to Zierhut et al.[38] Their main finding was that only TKER spectra recorded at wavelengths shorter than 233 nm display a fast structure, indicative of direct dissociation of the N9-H bond rather than statistical dissociation of a vibrationally hot molecule in the electronic ground state. According to their interpretation, prompt dissociation via the πσ* state does therefore not play a role at excitation wavelengths longer that 233 nm. Interestingly, these authors find a large background signal of slow H-atoms at all excitation wavelengths (214–280 nm) which is attributed to multi-photon excitation, even when using an unfocused pump laser. Finally, Wells et al.[40] reported a study of the fluence dependence of the adenine cation and proton signals in single-colour nano- and femtosecond ionization experiments using light at 266 nm. From the observation of an identical power-law for the fluence dependence in the nano- and femtosecond experiments, it was deduced that hydrogen atoms were produced and ionized within the cross-correlation of the laser pulses, thus necessitating the participation of the πσ* state. These experiments, however, cannot fully rule out the possibility that the protons may result from dissociative ionization rather than from processes in the neutral molecule.

7. Time-Resolved Photoelectron Spectroscopy

Our group used time-resolved photoelectron spectroscopy to obtain more information about the intermediate states involved in the electronic relaxation following UV excitation of

adenine and 9-methyladenine.[8–10] The TRPES spectra not only allowed us to consider the apparent nπ* and πσ* controversy, but also to investigate wavelength-dependent branching ratios for the different channels. In Figure 8 we compare the TRPES spectra of adenine and 9-methyladenine recorded at 267 nm excitation and 200 nm ionization. These spectra present photoelectron signals as a function of both time delay and photoelectron kinetic energy. The data are simultaneously fit at all
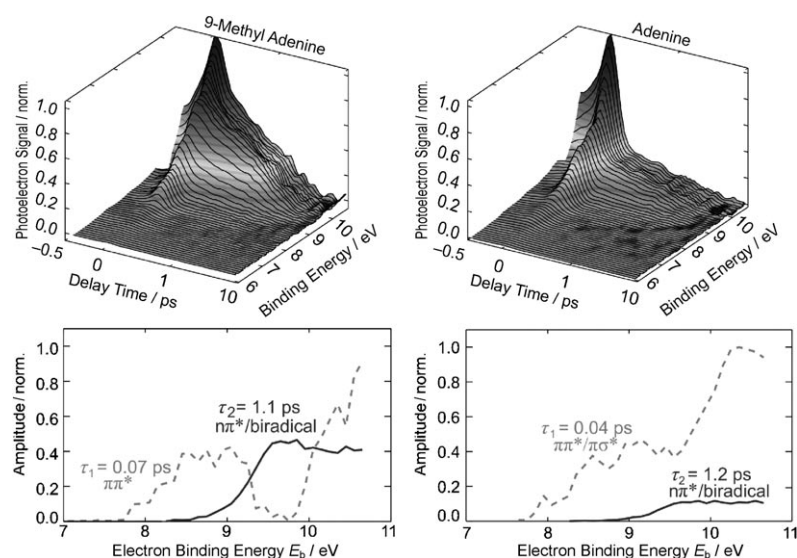
Figure 8. TRPES spectra of 9-methyladenine (left) and adenine (right) recorded at 267 nm pump and 200 nm probe. The decay-associated spectra of the fs and ps channels extracted from a biexponential global 2D fit are shown in the corresponding attached plots.

time delays and all electron kinetic energies using a bi-exponential model, allowing us to extract the decay-associated photoelectron spectra, that is, the time-independent spectrum of each time-component. Projection of the fit onto the energy axis (i.e. integration over delay times) yields the photoelectron spectrum of each relaxation channel. Projection onto the time axis (i.e. energy integration over each photoelectron channel) yields the time-dependent yield of each ionization channel. For both molecules the time evolution of the photoelectron spectra revealed two relaxation channels: a short-lived component ($t < 100$ fs) and one with a ps lifetime. The decay-associated spectra of the fast fs and slower ps channels are plotted below the two-dimensional data. For 9-methyladenine lifetimes of 70 fs and 1.1 ps are observed, compared to 40 fs and 1.2 ps in adenine, respectively. These numbers are in quantitative agreement with previous ion yield measurements where the similarity of these time-constants was used as evidence against the πσ* mechanism.[7] Nevertheless, significant differences between the decay channels in these two molecules are revealed in their associated photoelectron spectra. Their spectra associated with the fast decay component are qualitatively different and the relative amplitudes of the fast and the slow channel differ by a factor of four.

To aid the assignment of the different channels, we calculated Koopmans'-type ionization correlations for adenine (TD-

B3LYP/6-31++G**): S_1, the lowest $n\pi^*$ state, preferentially ionizes into the D_1 (n^{-1}) cation excited state, whereas S_2, the lowest $\pi\pi^*$ state, and S_3, a $\pi\sigma^*$ state, both preferentially ionize into the D_0 (π^{-1}) cation ground state and D_2 (π^{-1}). The corresponding vertical ionization potentials $IP_0 = 8.48$ eV, $IP_1 = 9.58$ eV, and $IP_2 = 10.5$ eV are known from He(I) photoelectron spectroscopy.[41] Absorption spectra, He(I) photoelectron spectra and calculated geometries for 9-methyladenine are very similar to those for adenine, but recent quantum chemical calculations indicate that a conical intersection between the $\pi\sigma^*$ state and the ground state might not be present along the N9-C stretch coordinate.[42] The same calculations also predict a significant barrier on the the $\pi\sigma^*$ potential along this coordinate. The decay-associated spectrum of the 1 ps component shows a similar shape for both molecules and, using Koopmans' ionization correlations, was assigned to ionization of the $n\pi^*$ state. This is direct spectroscopic evidence that the state with 1 ps lifetime is indeed the $n\pi^*$ state. By contrast, the decay-associated spectra of the <100 fs component show important spectral differences: in the 9.3–9.8 eV spectral region, adenine has non-zero amplitude that is absent in the 9-methyladenine spectrum. In the latter spectrum, the two distinct bands are located slightly above 8.5 eV and at 10.5 eV electron binding energy. These values match the energies expected for ionization into the D_0 (π^{-1}) and D_2 (π^{-1}) ionic states of 9-methyladenine and we therefore assign these bands to ionization of the initially excited $\pi\pi^*$ state. In adenine, we expect the contribution from the $\pi\pi^*$ to be very similar. However, the non-zero amplitude in the 9.3–9.8 eV binding energy region (between the two π^{-1} bands) strongly suggests that there is another short-lived state, which does not make any significant contribution in 9-methyladenine, but does so in adenine. We proposed that this could be the $\pi\sigma^*$ state which shares ionization correlations with the $\pi\pi^*$ state, but can be expected to have its spectrum broadened and shifted significantly by the large displacement along the N9-H bond. These arguments were supported by explicit Franck–Condon simulations.[10]

Based on the assumption that the difference in lifetime (40 fs compared to 70 fs) for the fast component in adenine and 9-methyladenine could be due to the presence of an additional channel in adenine, we can very roughly estimate its lifetime as 90 fs using a simple kinetic model. To determine the importance of the additional channel in adenine, we compare the relative amplitudes of the different channels for both molecules. The spectra displayed in Figure 8 are normalized to unit ionization yield for each molecule. The relative amplitude of the 1 ps component is reduced by a factor of four in adenine compared to 9-methyladenine and suggests that, in adenine, only approximately 25 % follows a sequential $\pi\pi^*$ to $n\pi^*$ decay path, with the majority proceeding via the additional channel. The reduced amplitude for the $n\pi^*$ channel matches the reduced branching to this channel predicted by the inclusion of a competing relaxation path having a lifetime of 90 fs. Therefore, this proposed kinetic model self-consistently matches both the lifetimes and the amplitudes. Our spectra show no evidence for any other significant relaxation pathways. For example, relaxation along another $\pi\sigma^*$ state at the NH_2 group or

a ring-opening mechanism, were it of any relevance, would be present in the photoelectron spectra of both adenine and 9-methyladenine. We cannot exclude these mechanisms based on our data alone, but the above-mentioned Franck–Condon simulations are consistent with the spectral changes in the 9.3–9.8 eV region being due to a $\pi\sigma^*$ at the 9-H position.

Our TRPES experiments cannot deduce what happens to the molecules if they reach the $\pi\sigma^*$ state. Along the N9-H stretch coordinate, the $\pi\sigma^*$ state has a conical intersection with the ground state. The possible outcomes of this crossing is either dissociation of the N9-H bond, creating a hydrogen atom and a ground state adeninyl radical, or a crossing back to the electronic ground state of adenine with high vibrational excitation. None of these products can be a single photon ionized at 200 nm. Based on the H-atom translational spectroscopy experiments by Nix et al.[39] we might propose that the latter mechanism holds at longer wavelengths.

Our attribution of the difference between adenine and 9-methyladenine to the $\pi\sigma^*$ relaxation path might be wrong; most high-level ab initio calculations indicate that the $\pi\pi^*/\pi\sigma^*$ conical intersection is not energetically accessible at 267 nm excitation, so although one may imagine trajectories on the lower cone leading from the $\pi\pi^*$ to the $\pi\sigma^*$ state, these calculations, together with the hydrogen-loss experiments from Nix et al.,[40] present a strong argument against the $\pi\sigma^*$ mechanism in this energy range. If indeed the $\pi\sigma^*$ model is inappropriate, some observations must still be explained by all other models. For instance, comparing adenine and 9-methyladenine, where the only difference is the substitution of a hydrogen atom with a methyl-group on the five-membered ring, the UV absorption spectra and He(I) photoelectron spectra are virtually indistinguishable, yet the time-resolved photoelectron spectra shows dramatic differences: 1) the yield of the $n\pi^*$ channel is reduced by a factor of four, 2) the photoelectron spectrum associated with the fast relaxation channel exhibits qualitative changes and 3) the time-constant for the fast channel changes in a way that together with the reduced $n\pi^*$ yield is self-consistently explained by the presence of another ultra-fast relaxation channel in adenine which is inoperative in 9-methyladenine. Since both the $n\pi^*$ and $\pi\pi^*$ relaxation paths primarily involve motion of atoms in the six-membered ring, it seems unlikely that these mechanisms should be strongly perturbed by methyl-substitution on the five-membered ring.

In a pump-wavelength-dependence study,[8] we compared TRPES spectra of adenine with 250 nm (see Figure 9) and 267 nm excitation, supporting the same picture as above for the relaxation dynamics. Lifetimes and decay associated spectra for both wavelengths and also for 9-methyladenine are similar. Based on the Koopmans ionization correlations mentioned above, the short-lifetime spectrum (shown in grey) was assigned to the S_2 ($\pi\pi^*$) state and the longer lifetime spectrum (in black) to the S_1 ($n\pi^*$) state. Compared to 267 nm excitation, the decay-associated spectra are shifted towards a slightly higher electron binding energy by 0.316 eV, the energy difference between 267 nm and 250 nm: higher vibrationally excited neutral excited states preferentially ionize into vibrationally excited cationic states ($\Delta v = 0$ propensity rule). The S_2 ($\pi\pi^*$) and
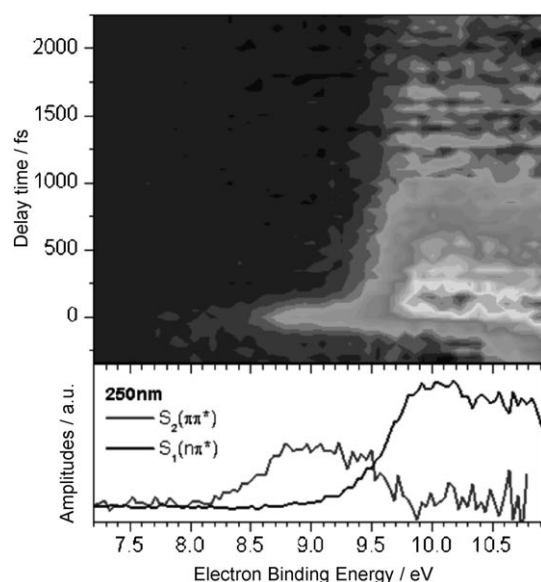
Figure 9. TRPES of adenine recorded at 250 nm pump and 200 nm probe along with the decay associated spectra of the fs and ps channels.

S_1 ($n\pi^*$) spectra correspond to lifetimes of < 50 fs and ~ 750 fs, respectively. Given the signal-to-noise ratio and associated uncertainties in the data fitting, these earlier values[8] and spectra are in good basic agreement with the more recent measurements.[43]

Comparing the ratio of the fast to slow components of the time-integrated photoelectron spectra at both wavelengths, we observed that the S_1 ($n\pi^*$) state amplitude at 250 nm is greatly enhanced compared to 267 nm excitation. Furthermore, the nominal S_2 ($\pi\pi^*$) spectrum shows subtle differences at high electron binding energies. At 250 nm excitation, the signal in the 9.8-10 eV energy region is insignificant and does not rise as steeply towards high electron binding energies as it does at 267 nm excitation. We speculated that these differences are associated with the operation of a $\pi\sigma^*$ state which, unfortunately, shares the same ionization correlations as the S_2 ($\pi\pi^*$) state. In the model derived from the wavelength dependence of the photoelectron spectra, the relative importance of relaxation via the $\pi\sigma^*$ channel state is strongly reduced at 250 nm excitation, due to the increase in the number of $\pi\pi^*$ to $n\pi^*$ decay pathways with increasing excitation energy. The existence of multiple $\pi\pi^*$–$n\pi^*$ conical intersections in DNA bases is discussed below.

Recently, Barbatti and Lischka[22] presented a set of mixed quantum-classical dynamics simulations designed to address the relaxation dynamics following excitation into the ^1L_a $\pi\pi^*$ (S_3) state of adenine. Their results revealed an ultrafast relaxation from the S_3 state via S_2 to the S_1 state within 60 fs followed by a much slower relaxation from S_1 to S_0 within 500 fs. These time-constants are in good agreement with the results of both the ion yield experiments of Canuel et al.[7] and our TRPES experiments. Barbatti and Lischka, however, claim that relaxation on the S_1 surface happens at the puckered ^2E geometry where the S_1 state has $\pi\pi^*$ character (the biradical state of Zgierski et al.[16]). This appears to contradict our assignment of

the slow component of the TRPES spectrum to the $n\pi^*$ state. One explanation may be that our use of the ionization correlations at the S_0 equilibrium geometry to assign the photoelectron spectrum could fail, since the excited ionic states may, just as the neutral states, interact strongly at bent geometries. High-level ab initio calculations of the Koopmans correlations could settle this point. This discrepancy, however, does not explain the differences between adenine and 9-methyladenine, since the distortions in the ^2E geometry are entirely located on the six-membered ring and thus should not be strongly affected by methyl substitution on the five-membered ring.

8. Conclusions

Following excitation into the strongly absorbing $\pi\pi^*$ state, the photophysics of the DNA base adenine is dominated by ultrafast electronic relaxation down to the ground electronic state. Ab initio calculations have predicted relaxation paths both directly from the initially excited state to the ground state and via other electronically excited states of $n\pi^*$ and $\pi\sigma^*$ character. A number of different experimental techniques have been invoked to identify the dominant relaxation processes. Several hydrogen-atom detection experiments have given a strong indication of relaxation via a $\pi\sigma^*$ state, but the energetic onset of the process is still disputed. In femtosecond pump–probe experiments, bi-exponential kinetics have been observed, indicating a two-step relaxation mechanism, the slow step of which has been assigned to relaxation from the $n\pi^*$ state.

TRPES studies on adenine and 9-methyladenine shed new light on the electronic states involved in the relaxation processes. Based on experimental and theoretical studies in the existing literature and supported by the pump wavelength dependence and methylation TRPES experiments described above, we summarize our current understanding of the electronic relaxation pathways in adenine as follows (see Figure 10, right): At 277 nm excitation, the minimum of the bright $\pi\pi^*$ state is reached which, due to the relative inaccessibility of the $n\pi^*$ and $\pi\sigma^*$ conical intersections, has a long lifetime of 9 ps— the relaxation process is explained by intersystem crossing. Following excitation at 267 nm, competing channels open up—an $n\pi^*$ channel plus an additional channel—with between 45–90 % proceeding via the additional channel. The lifetime of the additional channel was estimated to be 90 fs and the lifetime of the $n\pi^*$ state is 1.2 ps. At 250 nm excitation, the additional channel is still operational. However, the amplitude of the $S_2(\pi\pi^*)$ to $S_1(n\pi^*)$ channel is greatly enhanced due to accessibility of a larger number of higher-lying ring deformation modes that can provide access to multiple $\pi\pi^*$–$n\pi^*$ conical intersections. At the same time, the amplitude of the additional channel is not greatly affected. For 9-methyladenine (Figure 10, left) the additional channel is energetically unavailable and the relaxation back to the ground state occurs via the $n\pi^*$ state. Based on the arguments given above, we have proposed that this additional channel is the $\pi\sigma^*$ state. While current ab initio calculations are incompatible with this assignment, this model self-consistently explains all experimental observations.
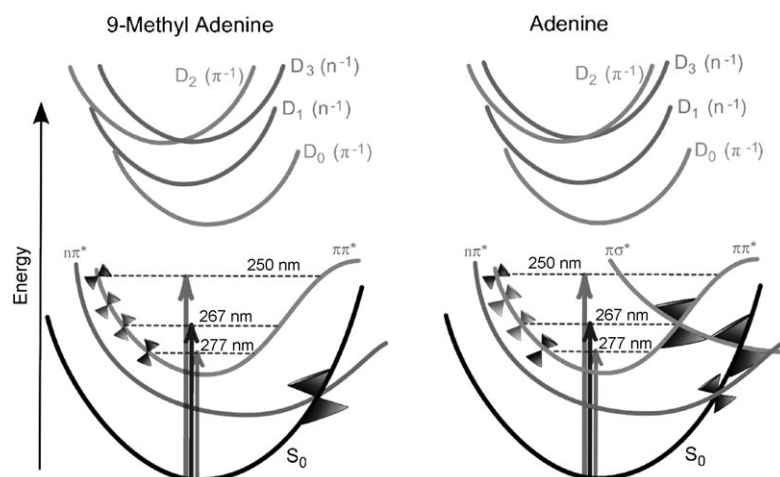
Figure 10. Schematic of the proposed electronic relaxation mechanism in 9-methyladenine (left) and adenine (right). The relative importance of the conical intersections is indicated by the size of the cones. Ionization correlations between the excited states and the energetically accessible cation states are shown by the grey-tone of the potential energy curves.

tions.[45] This behavior supports our explanation of the wavelength dependence of the relaxation dynamics in adenine. At the moment, such dynamics calculations remain challenging for a molecule the size of adenine.

10. Outlook

The studies on adenine compounds presented in this case study demonstrate the potential of time-resolved photoelectron spectroscopy for disentangling complex relaxation pathways in isolated molecules. We foresee opportunities for this technique in the study of a variety of small biomolecular building blocks. In direct continuation of our adenine work, we have also studied thymine and uracil using a combination of time-resolved photoelectron spectroscopy and ab initio molecular dynamics calculations. Both thymine and uracil show a multi-exponential decay involving an ultrafast < 50 fs component, an intermediate 3.9 ps (thymine) and 1.8 ps (uracil) component, and a long-lived nanosecond component. A surprisingly large effect is seen in the ps lifetime of thymine and uracil which differ only by the presence of a methyl group in thymine. Using an ab initio multiple spawning (AIMS) method, Hudock et al.[44] showed that the fs decay corresponds to relaxation to an S_2 minimum. Responsible for the ps component is a barrier crossing on the S_2 surface to the S_2/S_1 conical intersection which involves out-of plane motion of the H or CH_3, in uracil and thymine, respectively, and hence explains the difference in the ps lifetimes. It is worth noting that, for both molecules, a barrierless path exists from the Franck–Condon region to the S_2/S_1 conical intersection, yet the ultrafast time-constant is related to nuclear dynamics on a single electronic surface, because the gradient in a mass-weighted coordinate system points towards the S_2 minimum. We have also recorded preliminary time-resolved photoelectron spectra of cytosine, but the interpretation of the data is complicated by the presence of two tautomers in the molecular beam. For this molecule, very recent AIMS calculations showed the surprising result that no single path dominates the relaxation, but rather that a large number of independent paths make significant contribu-

[1] C. E. Crespo-Hernández, B. Cohen, P. M. Hare, B. Kohler, *Chem. Rev.* **2004**, *104*, 1977.
[2] M. Klessinger, J. Michl, *Excited States and Photochemistry of Organic Molecules*, VCH, Weinheim, **1995**.
[3] C. E. Crespo-Hernández, B. Cohen, B. Kohler, *Nature* **2005**, *436*, 1141.
[4] A. Broo, *J. Phys. Chem. A* **1998**, *102*, 526.
[5] H. Kang, K. T. Lee, B. Jung, Y. J. Ko, S. K. Kim, *J. Am. Chem. Soc.* **2002**, *124*, 12958.
[6] A. L. Sobolewski, W. Domcke, *Eur. Phys. J. D* **2002**, *20*, 369.
[7] C. Canuel, M. Mons, F. Piuzzi, B. Tardivel, I. Dimicoli, M. Elhanine, *J. Chem. Phys.* **2005**, *122*, 074316.
[8] S. Ullrich, T. Schultz, M. Z. Zgierski, A. Stolow, *J. Am. Chem. Soc.* **2004**, *126*, 2262.
[9] S. Ullrich, T. Schultz, M. Z. Zgierski, A. Stolow, *Phys. Chem. Chem. Phys.* **2004**, *6*, 2796.
[10] H. Satzger, D. Townsend, M. Z. Zgierski, S. Patchkovskii, S. Ullrich, A. Stolow, *Proc. Natl. Acad. Sci. USA* **2006**, *103*, 10196.
[11] A. Stolow, *Annu. Rev. Phys. Chem.* **2003**, *54*, 89.
[12] A. Stolow, A. E. Bragg, D. M. Neumark, *Chem. Rev.* **2004**, *104*, 1719.
[13] J. G. Underwood, A. Stolow, *Adv. Chem. Phys.* **2008**, *139*, 497.
[14] V. Blanchet, M. Z. Zgierki, T. Seideman, A. Stolow, *Nature* **1999**, *401*, 52.
[15] J. Lin, C. Yu, S. Peng, I. Akiyama, K. Li, L. K. Lee, P. R. LeBreton, *J. Am. Chem. Soc.* **1980**, *102*, 4627.
[16] M. Z. Zgierski, S. Patchkovskii, E. C. Lim, *Can. J. Chem.* **2007**, *85*, 124.
[17] M. P. Fülscher, L. Serrano-Andrés, B. O. Roos, *J. Am. Chem. Soc.* **1997**, *119*, 6168.
[18] S. K. Mishra, M. K. Shukla, P. C. Mishra, *Spectrochim. Acta Part A* **2000**, *56*, 1355.
[19] A. Holmén, A. Broo, B. Albinsson, B. Nordén, *J. Am. Chem. Soc.* **1997**, *119*, 12240.
[20] B. Mennucci, A. Toniolo, J. Tomasi, *J. Phys. Chem. A* **2001**, *105*, 4749.
[21] L. Serrano-Andrés, M. Merchán, A. C. Borin, *Proc. Natl. Acad. Sci. USA* **2006**, *103*, 8691.
[22] M. Barbatti, H. Lischka, *J. Am. Chem. Soc.* **2008**, *130*, 6831.
[23] L. B. Clark, G. G. Peschel, I. Tinoco, Jr., *J. Phys. Chem.* **1965**, *69*, 3615.
[24] N. J. Kim, G. Jeong, Y. S. Kim, J. Sung, S. K. Kim, Y. D. Park, *J. Chem. Phys.* **2000**, *113*, 10051.
[25] D. C. Lührs, J. Viallon, I. Fischer, *Phys. Chem. Chem. Phys.* **2001**, *3*, 1827.
[26] E. Nir, C. Plützer, K. Kleinermanns, M. de Vries, *Eur. Phys. J. D* **2002**, *20*, 317.
[27] C. Plützer, K. Kleinermanns, *Phys. Chem. Chem. Phys.* **2002**, *4*, 4877.
[28] C. Plützer, E. Nir, M. S. de Vries, K. Kleinermanns, *Phys. Chem. Chem. Phys.* **2001**, *3*, 5466.
[29] T. Zwier, *J. Phys. Chem. A* **2001**, *105*, 8827.
[30] S. Perun, A. L. Sobolewski, W. Domcke, *Chem. Phys.* **2005**, *313*, 107.

[31] C. M. Marian, *J. Chem. Phys.* **2005**, *122*, 104314.

[32] S. Perun, A. L. Sobolewski, W. Domcke, *J. Am. Chem. Soc.* **2005**, *127*, 6257.

[33] H. Chen, S. Li. , *J. Phys. Chem. A* **2005**, *109*, 8443.

[34] L. Blancafort, *J. Am. Chem. Soc.* **2006**, *128*, 210.

[35] T. J. Martínez, *Acc. Chem. Res.* **2006**, *39*, 119.

[36] H. Kang, B. Jung, S. K. Kim, *J. Chem. Phys.* **2003**, *118*, 6717.

[37] I. Hünig, C. Plützer, K. A. Seefeld, D. Löwenich, M. Nispel, K. Kleinermanns, *ChemPhysChem* **2004**, *5*, 1427.

[38] M. Zierhut, W. Roth, I. Fischer, *Phys. Chem. Chem. Phys.* **2004**, *6*, 5178.

[39] M. G. D. Nix, A. L. Devine, B. Cronin, M. N. R. Ashfold, *J. Chem. Phys.* **2007**, *126*, 124312.

[40] K. L. Wells, G. M. Roberts, V. G. Stavros, *Chem. Phys. Lett.* **2007**, *446*, 20.

[41] S. Peng, A. Padva, P. R. LeBreton, *Proc. Natl. Acad. Sci. USA* **1976**, *73*, 2966.

[42] S. Brønsted Nielsen, T. I. Sølling, *ChemPhysChem* **2005**, *6*, 1276.

[43] The contribution from a "ns" component reported in refs. [8,9] is minor and might possibly be associated with the presence of the 7H-adenine tautomer. Conflicting observations regarding the tautomer ratio have been reported by different groups (see Introduction) that suggest a dependence on the experimental conditions.

[44] H. R. Hudock, B. G. Levine, A. L. Thompson, H. Satzger, D. Townsend, N. Gador, S. Ullrich, A. Stolow, T. J. Martínez, *J. Phys. Chem. A* **2007**, *111*, 8500.

[45] H. R. Hudock, T. J. Martínez, *Angew. Chem.* **2008**, DOI: 10.1002/ange.200801250*Angew. Chem. Int. Ed.* **2008**, DOI: 10.1002/anie.200801250.